High-Speed Silicon-Organic Hybrid (SOH) Modulator with 1.6 fJ/bit and 180 pm/V In-Device Nonlinearity

R. Palmer[1], S. Koeber[1], W. Heni[1], D. L. Elder[2], D. Korn[1], H. Yu[3], L. Alloatti[1], S. Koenig[1], P. C. Schindler[1], W. Bogaerts[3], M. Pantouvaki[4], G. Lepage[4], P. Verheyen[4], J. Van Campenhout[4], P. Absil[4], R. Baets[3], L. R. Dalton[2], W. Freude[1], J. Leuthold[1,5], C. Koos[1]

(1) Karlsruhe Institute of Technology (KIT), Institutes IPQ and IMT, 76131 Karlsruhe, Germany, robert.palmer@kit.edu, christian.koos@kit.edu
(2) University of Washington, Department of Chemistry, Seattle, WA 98195-1700, United States
(3) Ghent University – IMEC, Photonics Research Group, Gent, Belgium
(4) IMEC vzw. Kapeldreef 75, Heverlee, Belgium
(5) Electromagnetic Fields & Microwave Electronics Laboratory (IFH), ETH-Zurich, Zurich, Switzerland

Abstract *We report on a 40 Gbit/s silicon-organic hybrid (SOH) modulator with 11 dB extinction ratio. A novel electro-optic chromophore with record in-device nonlinearity of 180 pm/V leads to* $V_\pi L$ *= 0.5 Vmm and a low energy consumption of 1.6 fJ/bit at 12.5 Gbit/s.*

Introduction

Energy-efficient silicon electro-optic modulators are key components for future short-distance interconnects in data centers and high-performance computers [1]. Targeted energy consumptions are tens of fJ/bit for dense off-chip connections, and a few fJ/bit for global on-chip connections [1]. Over the last years, a variety of silicon modulators has been demonstrated based on free-carrier depletion, or injection in pn-diodes, or based on metal-oxide-semiconductor (MOS) structures [2, 3]. Carrier injection devices have typically very small voltage-length products of $V_\pi L$ = 0.36 V mm [4], but the large carrier lifetime calls for pre-emphasis and limits the modulation speed to 20 GHz. The modulation energy per bit is usually in the pJ-range due to the forward bias of the diode. Carrier depletion modulators, in contrast, have been demonstrated to operate at data rates of up to 50 Gbit/s [5], but typically with $V_\pi L$ > 10 Vmm for non-resonant devices. Extinction ratios (ER) range from 3 dB to 8 dB at high data rates, and the lowest reported energy consumption is 200 fJ/bit [6]. Modulation energies can be significantly reduced by using resonant structures, such as ring resonators, microdisks or photonic crystal waveguides. The lowest energy consumption reported to date for a silicon-based modulator amounts to 3 fJ/bit and has been achieved with a microdisk modulator operated at a data rate of 12.5 Gbit/s with a drive voltage of 1 V_{pp} and an ER of 3.2 dB [7]. However, both carrier injection and depletion type modulators are subject to an inherent coupling of amplitude and phase modulation, and resonant structures suffer from strong wavelength dependence and temperature sensitivity.

In this paper, we pursue a fundamentally different approach by combining silicon slot waveguides with electro-optic cladding materials in a non-resonant silicon-organic hybrid (SOH) device. Pure phase modulation is achieved by exploiting the linear electro-optic effect in the cladding, where we reached an in-device material nonlinearity of r_{33} = (180±20) pm/V – the highest in-device value reported so far. For a 1 mm long device this leads to a π-voltage of V_π = 0.5 V measured at DC. At 12.5 Gbit/s we demonstrate data transmission with record-low peak-to-peak drive voltages of 125 mV_{pp}, corresponding to an energy consumption of 1.6 fJ/bit. This is, to the best of our knowledge, the lowest energy consumption reported so far for silicon-based MZI modulators, a value that compares well even with best-in-class resonant devices. We further show that our device can be operated at symbol rates of at least 40 GBd, where an ER of better than 10 dB is achieved.

Silicon-Organic Hybrid Modulator

The schematic of a phase modulator is depicted in Fig. 1(a). It consists of a slot waveguide electrically connected to a coplanar transmission line through 60 nm thick doped silicon strips. The voltage applied to the transmission line drops across the narrow slot, resulting in a high electric field that strongly overlaps with the optical mode, Fig. 1(a). The waveguide is covered and the slot is filled with the electro-optic chromophore DLD164, see inset of Fig. 1(a). The cladding is applied to the chip by spin coating a solution of 8% DLD164 dissolved in 1,1,2-trichloroethane. The cladding refractive index is n = 1.83 at λ = 1550 nm. Earlier approaches to SOH integration of $\chi^{(2)}$-nonlinear molecules [8, 9] utilized a limited percentage of dipolar chromophore dopants in an inert polymeric host matrix. Here, in contrast, we do not use a polymer matrix. Instead, the monolithic chromophore

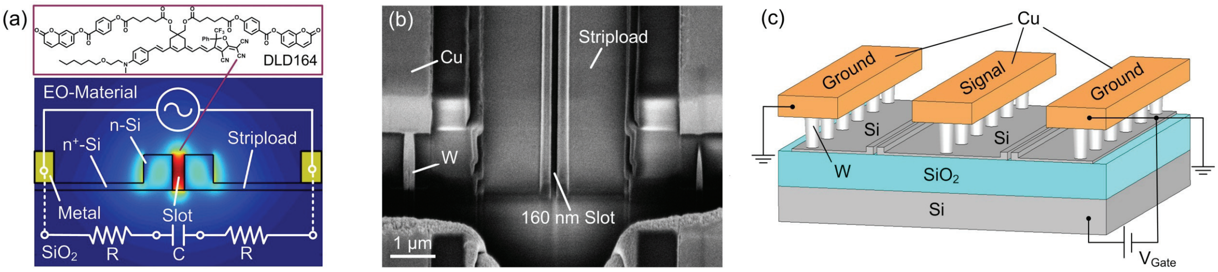

Fig. 1: (a) Schematic and simulated optical mode of a phase-modulator with chemical structure of the nonlinear chromophore. The two rails of a silicon slot waveguide are electrically connected to metal electrodes by 60 nm high *n*-doped (As, $4 \times 10^{17} cm^{-3}$) silicon slabs. The modulation voltage drops over the narrow slot resulting in a high modulation field that has a strong overlap with the optical mode. The novel highly nonlinear chromophore DLD164 is used as an electro-optic cladding material. (b) SEM image of a fabricated phase modulator. Copper electrodes are connected to the slot waveguide by tungsten vias. (c) Schematic of the MZI modulator. The device is driven in push-pull by a coplanar transmission line (ground-signal-ground). A gate voltage is applied at the silicon substrate to increase the conductivity of the silicon slab region [9].

bearing pendant coumarin side groups is applied to the slot waveguide. These side groups both stabilize the glassy matrix and significantly enhance the poling efficiency [10].

Silicon waveguides are fabricated in IMEC by 193 nm deep-UV lithography on a 220 nm SOI wafer with a 2 µm thick buried oxide. The Mach-Zehnder interferometer (MZI) modulator, Fig. 1(c), consists of an MZI with two identical 1 mm long phase-modulators, Fig. 1(a). The two phase modulators are driven in push-pull operation by a coplanar waveguide (CPW, ground-signal-ground, GSG) as depicted in Fig. 1(c). The CPW consists of 600 nm thick copper lanes linked to the silicon modulator by 900 nm thick tungsten vias. The metallization stack is locally opened to expose the slot waveguide. Fig. 1(b) shows an SEM image of the fabricated phase modulator with its metal stack. We measure a slot width of 160 nm and a rail width of 210 nm. The electro-optic cladding is poled at elevated temperatures by applying a DC voltage across the ground electrodes. The voltage-length product of the MZI modulator was measured to be $V_\pi L = 0.5$ Vmm in the low-frequency limit. Taking into account the measured waveguide dimensions we calculate the corresponding in-device nonlinearity of the cladding to be $r_{33} = (180 \pm 20)$ pm/V. The fiber-to-fiber loss is 16.5 dB. The on-chip loss is approximately 6 dB for maximum transmission of the modulator.

On-Off Keying Experiments

A pseudorandom bit pattern generator (PPG) with a PRBS length of 2^{31}-1 drives the MZI modulator using a GSG picoprobe. A bias voltage of 2 V is applied at the same GSG electrodes by using a bias-T. A 50 Ω resistor terminates the CPW via a second picoprobe. Light from an external cavity laser (1550 nm, 5 dBm) is coupled to the silicon chip and modulated. The data signal is amplified and fed to a digital communications analyzer (DCA) and a bit-error ratio (BER) tester. A gate field of up to 250 V/µm is applied as depicted in Fig. 1(c) for increasing the conductivity of the thin silicon slabs [9]. Fig. 2 depicts NRZ OOK eye diagrams for data rates between 12.5 Gbit/s and 40 Gbit/s at a drive voltage of 950 mV_{pp}. The ER exceeds 10 dB for all data rates. At 12.5 Gbit/s and 30 Gbit/s we measure Q²-factors of 22 dB and 19 dB, respectively, and the BER is below 1×10^{-11}. At 40 Gbit/s we measure a Q² of 15 dB and a BER of 1×10^{-8}. In a second experiment, we reduce the drive voltage of the modulator. Measured BER are depicted in Fig. 3(a) for data rates of 12.5 Gbit/s and 25 Gbit/s. The measured BER stays below the hard-decision 2nd generation FEC threshold of BER = 2.3×10^{-3} for drive voltages of 190 mV_{pp} (7 fJ/bit) and 150 mV_{pp} (9 fJ/bit) for 25 Gbit/s and 12.5 Gbit/s, respectively, when the modulator CPW is terminated. Due to the short 1 mm length, the device can also be operated without termination ("lumped") at a data rate of 12.5 Gbit/s.

Next, we estimate the energy consumption of the modulator. As common in the field, we do this by calculating the dissipated RF power. Therefore, power consumption of laser, optical amplifier and electrical drivers is not included in these numbers. The estimated energy consump-

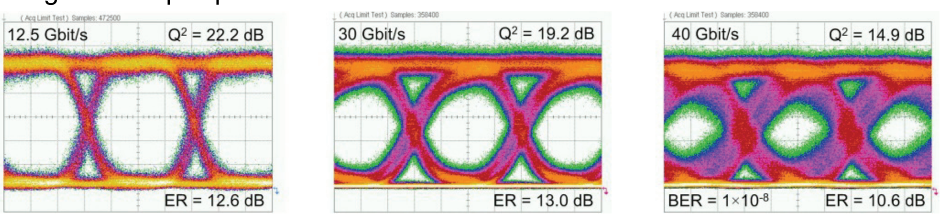

Fig. 2 NRZ OOK eye diagrams at 12.5 Gbit/s, 30 Gbit/s and 40 Gbit/s measured at quadrature. Q²-factors, extinction ratios (ER) and bit error ratios (BER) are denoted in the figure. Drive voltage 950 mV_{pp}. The ER exceeds 10 dB up to 40 Gbit/s. No bit errors are measured at 12.5 Gbit/s and 30 Gbit/s. At 40 Gbit/s we measure a BER of 1×10^{-8}. PRBS length 2^{31}-1.

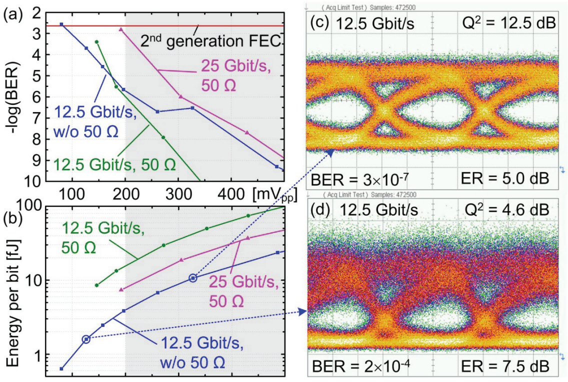

Fig. 3 Eye diagram and energy consumption of the modulator when operated at low drive voltages. (a) Measured BER as a function of drive voltage for data rates of 12.5 Gbit/s and 25 Gbit/s when the DUT is terminated by a 50 Ω probe (green, magenta) and for a rate of 12.5 Gbit/s for an unterminated device. Data points in the gray colored area were measured at quadrature. (b) Corresponding energy per bit for the various drive voltages of (a). (c) Optical eye diagram at 12.5 Gbit/s for an unterminated device at quadrature; V_{drive} = 320 mV_{pp}, W_{bit}=10 fJ. (d) Optical eye diagram at 12.5 Gbit/s for an unterminated device below quadrature; V_{drive} = 125 mV_{pp}, W_{bit}=1.6 fJ.

tion for various transmission experiments and for different peak-to-peak drive voltages V_{drive} is plotted in Fig. 3(b). The values have been derived as follows. For the 50 Ω-terminated device, and assuming an ideally rectangular NRZ drive voltage, the energy W_{bit} per bit is estimated by dividing the electrical input power by the data rate r, $W_{bit} = (V_{drive}/2)^2/50\Omega/r$. For the unterminated device, we estimate the power dissipation associated with (dis-)charging the total capacitance C_{mod} of the modulator as seen by the CPW to be $W_{bit} = C_{mod} \times V_{drive}^2/4$ [1]. Crucial parameters are the drive voltage and the modulator capacitance. For the terminated device, V_{drive} is measured with a 50 Ω-terminated scope before connecting the RF-cable to the Picoprobe. For the unterminated device, V_{drive} must be inferred. To this end, the frequency-dependent input impedance Z_{in} is measured with a vector network analyzer (VNA). With the measured open-circuit generator voltage $2V_{scope}$, the frequency dependent voltage V_{drive} can then be calculated. For finding the average of $\left|V_{drive}^2(f)\right|$, we weigh with a $\sin^2(\pi f/r)/(\pi f/r)^2$ function (assuming rectangularly-shaped pulses) and integrate over the relevant frequency range. From this we calculate the mean voltage $\overline{V_{drive}} = 1.8 \cdot V_{scope}$. Furthermore we extract the modulator capacitance from $Z_{in}(f)$ and find $C_{mod} = 2C = (400 \pm 20)\mathrm{fF}$ in good agreement with values predicted by an electrostatic simulation (CST). Furthermore we check the capacity by measuring devices of different length (250 µm to 1.5 mm) and confirm a linear relation between length and C_{mod}.

Currents flowing due to bias and gate voltages are measured to be below 2 nA and below 100 fA, respectively, contributing a negligible energy consumption of less than 1 aJ/bit. For a drive voltage such that we remain below the FEC-threshold in Fig. 3(a), the lowest energy-per-bit value is (1.6 ± 0.1) fJ/bit. This is obtained for an unterminated modulator operated at a mean drive voltage of 125 mV_{pp} (V_{scope} = 70 mV_{pp}) at a data rate of 12.5 Gbit/s. At 80 mV_{pp} drive voltage, a BER of 2.7×10^{-3} is measured, still very near the hard-decision (and certainly below the soft-decision) FEC threshold with an energy consumption of only 0.6 fJ/bit. These are the lowest values reported so far for nonresonant silicon modulators, comparing well with the energy required by resonant structures.

Conclusions

We experimentally demonstrate a high-speed silicon-organic push-pull MZI modulator with a very low energy consumption of 1.6 fJ/bit. The device is successfully operated at data rates up to 40 Gbit/s. Drive voltages can be as low as 125 mV_{pp} due to hybridization of a silicon slot waveguide and a novel highly nonlinear organic chromophore that has an in-device nonlinearity of $r_{33} = (180 \pm 20)$ pm/V after poling.

Acknowledgements

We acknowledge support by the DFG Center for Functional Nanostructures (CFN), the Karlsruhe International Research School on Teratronics (HIRST), the Karlsruhe School of Optics and Photonics (KSOP), the Initiative and Networking Fund of the Helmholtz Association, the DFG Major Research Instrumentation Programme, the Alfried Krupp von Bohlen und Halbach Foundation, the EU-FP7 projects SOFI, OTONES, PHOXTROT and by the BMBF joint project MISTRAL, the European Research Council (Starting Grant 'EnTeraPIC', no. 280145), the National Science Foundation (DMR-0905686, DMR-0120967) and the Air Force Office of Scientific Research (FA9550-09-1-0682), the Karlsruhe Nano-Micro Facility (KNMF), the Light Technology Institute (KIT-LTI) and ePIXfab (silicon photonics platform). We are grateful to P. Brenner (KIT-CFN) for support in nano-inspection and analysis and to P. Pahl (KIT-IHE) for support in RF-analysis.

References

[1] D. A. B. Miller, Opt. Express, 20(S2), 2012.
[2] G. T. Reed, et al., Nature Photon., 4:518–526, 2010.
[3] J. Fujikata, et al., OFC 2010, paper OMI3.
[4] W. M. Green, et al., Opt. Express, 15(25):17106–17113, 2007.
[5] D.J. Thomson, et al., Photon. Technol. Lett., 24(4):234–236, 2012.
[6] T. Baehr-Jones, et al., Opt. Express, 20(11):12014–12020, 2012.
[7] M. R. Watts, et al., Opt. Express, 19(22):21989–22003, 2011.
[8] R. Ding, et al., J. Lightwave Technol., 29(8):1112–1117, 2011.
[9] L. Alloatti, et al., Opt. Express, 19(12):11841–11851, 2011.
[10] S. J. Benight, et al. J Phys. Chem. B, 114(37):11949–11956, 2010.